

# LONGITUDINAL DISPLACEMENT OF THE CAROTID WALL AND CARDIOVASCULAR RISK FACTORS: ASSOCIATIONS WITH AGING, ADIPOSITY, BLOOD PRESSURE AND PERIODONTAL DISEASE INDEPENDENT OF CROSS-SECTIONAL DISTENSIBILITY AND INTIMA-MEDIA THICKNESS

GUILLAUME ZAHND<sup>1</sup>, DIDIER VRAY<sup>1</sup>, ANDRE SERUSCLAT<sup>2</sup>, DJHIANNE ALIBAY<sup>2</sup>, MARK BARTOLD<sup>3</sup>, ALEX BROWN<sup>4</sup>, MARION DURAND<sup>5</sup>, LISA M. JAMIESON<sup>6</sup>, KOSTAS KAPELLAS<sup>6</sup>, LOUISE J. MAPLE-BROWN<sup>7</sup>, KERIN O'DEA<sup>8</sup>, PHILIPPE MOULIN<sup>5,9</sup>, DAVID S. CELERMAJER<sup>10</sup>, MICHAEL R. SKILTON<sup>11</sup>

<sup>1</sup>Universite de Lyon, CREATIS, CNRS UMR 5220, INSERM U1044, INSA, Lyon, France

<sup>2</sup>Department of Radiology, Louis Pradel Hospital, Lyon, France

<sup>3</sup>Colgate Australian Clinical Dental Research Centre, School of Dentistry, University of Adelaide, Adelaide, Australia

<sup>4</sup>Baker IDI Heart and Diabetes Institute, Alice Springs, Australia

<sup>5</sup>Department of Endocrinology, Louis Pradel Hospital, Hospices Civils de Lyon, Universite Lyon1, Lyon, France

<sup>6</sup>Australian Research Centre for Population Oral Health, School of Dentistry, University of Adelaide, Adelaide, Australia

<sup>7</sup>Menzies School of Health Research, Charles Darwin University, Darwin, Australia

<sup>8</sup>Sansom Institute for Health Research, UniSA, Adelaide, Australia

<sup>9</sup>INSERM UMR 1060, Lyon, France

<sup>10</sup>Department of Medicine, University of Sydney

<sup>11</sup>Boden Institute of Obesity, Nutrition, Exercise and Eating Disorders, University of Sydney

*Manuscript published in Ultrasound in Medicine and Biology*

*(DOI: 10.1016/j.ultrasmedbio.2012.05.004).*

*The final version of the paper is available at:*

*<http://www.sciencedirect.com/science/article/pii/S0301562912002803>*

## **Abstract**

The recently discovered longitudinal displacement of the common carotid arterial wall (i.e., the motion along the same plane as the blood flow), may be associated with incident cardiovascular events and represents a novel and relevant clinical information. At present, there have only been a few studies that have been conducted to investigate this longitudinal movement. We propose here a method to assess noninvasively the wall bi-dimensional (two-dimensional [2-D], cross-sectional and longitudinal) motion and present an original approach that combines a robust speckle tracking scheme to guidance by minimal path contours segmentation. Our method is well suited to large clinical population studies as it does not necessitate strong imaging prerequisites. The aim of this study is to describe the association between the longitudinal displacement of the carotid arterial wall and cardiovascular risk factors, among which periodontal disease. Some 126 Indigenous Australians with periodontal disease, an emerging risk factor, and 27 healthy age- and sex-matched non-indigenous control subjects had high-resolution ultrasound scans of the common carotid artery. Carotid intima-media thickness and arterial wall 2-D motion were then assessed using our method in ultrasound B-mode sequences. Carotid longitudinal displacement was markedly lower in the periodontal disease group than the control group (geometric mean (IQR): 0.15 mm (0.13) vs. 0.42 mm (0.30), respectively;  $p < 0.0001$ ), independent of

cardiovascular risk factors, cross-sectional distensibility and carotid intima-media thickness ( $p < 0.0001$ ). A multivariable model indicated that the strongest correlates of carotid longitudinal displacement in adults with periodontal disease were age (b-coefficient = 2.235,  $p = .03$ ), waist (b-coefficient = 2.357,  $p = 0.001$ ), and pulse pressure (b-coefficient = .175,  $p = 0.07$ ), independent of other cardiovascular risk factors, cross-sectional distensibility and pulse wave velocity. Carotid longitudinal displacement, estimated with our approach, is impaired in the periodontal disease group, independent of established cardiovascular risk factors and other noninvasive measures of arterial stiffness, and may represent an important marker of cardiovascular risk.

**Key Words:** Arterial stiffness, Atherosclerosis, B-mode ultrasound, Cardiovascular risk factors, Carotid artery, Longitudinal displacement, Motion estimation, Periodontal disease, Segmentation, Speckle tracking.

Address correspondence to: Guillaume Zahnd, CREATIS, INSA Lyon, Bat. Blaise Pascal, 7 Av. Jean Capelle, 69621 Villeurbanne Cedex, France.

E-mail: guillaume.zahnd@creatis.insa-lyon.fr or michael.skilton@sydney.edu.au

## INTRODUCTION

Alterations in vascular dynamics, including arterial stiffening, are present decades prior to the onset of clinical cardiovascular events (Celermajer et al. 1992; Whincup et al. 2005) and appear to be predictive of cardiovascular events independent of traditional risk factors (Laurent et al. 2001; Weber et al. 2004; Dolan et al. 2006). Cross-sectional (i.e. radial) stiffness is a strong contributor to arterial pulse wave velocity (PWV), the current gold standard measure of arterial stiffness. Accordingly, the assessment of diameter change of the common carotid artery through the cardiac cycle is widely used as a measure of localized arterial stiffness (Gamble et al. 1994; Hansen et al. 1995; Jiang et al. 2000).

Nonetheless, these classical methods cannot directly capture the information concerning the specific movement of the arterial wall in the same orientation as the blood. Such longitudinal displacement of the intima-media complex tissues is less likely to influence arterial PWV, however, it may provide relevant additional information concerning arterial stiffness and vascular health than that derived from established methods. Longitudinal displacement of the human arterial wall and its physiologic implications have been characterized by recent studies, namely this phenomenon (1) can be measured noninvasively with precision (Cinthio et al. 2005); (2) has been detailed as a complex triphasic motion pattern with a larger movement against the blood flow during systole and being of the same magnitude as the radial motion (Cinthio et al. 2006); (3) has been demonstrated to be reduced in patients with carotid plaques, coronary artery disease and type 2 diabetes (Svedlund and Gan 2011a, 2011b; Zahnd et al. 2011a); (4) may be predictive of incident cardiovascular events independent of carotid stiffness and carotid atherosclerosis (Svedlund et al. 2011); and, (5) in pigs, undergoes profound changes in response to catecholamines (Ahlgren et al. 2011).

Periodontal disease, an inflammatory disease of the tissues surrounding the teeth, is an emerging independent cardiovascular risk factor (Scannapieco et al. 2003; Bouchard et al. 2010). Periodontal disease is associated with preclinical measures of vascular health including increased subclinical atherosclerosis and arterial endothelial dysfunction (Amar et al. 2003; Beck et al. 2011) but not PWV (Miyaki et al. 2006; Franek et al. 2009). Accordingly, we sought to determine whether carotid longitudinal displacement is altered in adults with periodontal disease, compared with age- and sex-matched healthy control subjects. The periodontal disease group was made up of Indigenous Australians with moderate to severe periodontal disease enrolled in the PerioCardio study (Skilton et al. 2011). Indigenous Australians are at increased risk of premature cardiovascular disease, predominantly

because of increased burden of established and emerging cardiovascular risk factors, as opposed to being Indigenous per se (O’Dea 1991; Brown et al. 2005). Additionally, periodontal disease is associated with elevated total cholesterol and low high-density lipoprotein cholesterol (HDL-c) (Wu et al. 2000; Buhlin et al. 2003). Thus, we also sought to determine whether any observed difference in carotid longitudinal displacement between the periodontal disease and control groups was potentially because of differences in established cardiovascular risk factors. We also described the association of cardiovascular risk factors with carotid longitudinal displacement within adults with periodontal disease, to further describe the association of specific risk factors and carotid longitudinal displacement.

## **MATERIALS AND METHODS**

**Study populations** Subjects with periodontal disease were participants in the PerioCardio study, described in detail elsewhere (Skilton et al. 2011). These participants are Indigenous Australians with moderate to severe periodontal disease, aged  $\geq 25$  years, with no known history of cardiovascular disease. The first 126 participants recruited into the PerioCardio study were included in this analysis. One participant had ultrasound scans of insufficient quality to enable assessment of longitudinal displacement (i.e., the interfaces of both walls could not clearly be seen because of the image noise) and, thus, was excluded from analysis.

As a control group, we included 27 age- and sex-matched healthy volunteers from Lyon, France, who were part of a larger study conducted by ourselves and others, in which carotid longitudinal displacement was ascertained using the same technique. Control subjects were healthy, non-smoking adults with no prior history of cardiovascular risk factors (hypercholesterolemia, diabetes, hypertension or family history of cardiovascular events).

Table 1 displays participant characteristics for the periodontal disease and control groups. Informed consent was obtained from all participants and the study was approved by appropriate institutional ethics committees in both Australia (Menzies School of Health Research, Northern Territory Department of Health Human Research Ethics Committee, Central Australian Human Research Ethics Committee, Northern Territory Correctional Services Research Committee, University of Adelaide Human Research Ethics Committee and the Aboriginal Health Council of South Australia) and France (Sud-Est committee).

### *Acquisition of the carotid artery ultrasound sequences*

Ultrasound images for the periodontal disease group were obtained using a portable ultrasound (Sonosite MicroMaxx, Bothell, WA, USA), with a 10–5 MHz linear array transducer, as previously described (Skilton et al. 2011). The B-mode sequence frame rate was 45 fps and the pixel size was 47 mm in both radial and longitudinal directions. Multiple loops of approximately six cardiac cycles duration were obtained for both the right and left common carotid arteries of each participant. For 17 participants, only ultrasound stills, as opposed to loops, were available from the baseline visit and, as such, ultrasound sequences from the 3-month visit were used for these participants.

Ultrasound images for the control group were obtained using a mainframe ultrasound scanner (ACUSON Antares premium edition; Siemens, Erlangen, Germany) equipped with a 10–5 MHz linear array transducer. The B-mode sequence frame rate was 29 fps and the pixel size was 30 mm in both radial and longitudinal directions. For the control group, longitudinal displacement was assessed from a single loop consisting of two to three cardiac cycles obtained from the left common carotid artery.

## *Estimation of the two-dimensional carotid wall displacement: cross-sectional and longitudinal motion*

All the processing, for both study populations, was conducted offline on a workstation at a central reading site by the same operator (G.Z.). We used a dedicated software method (Carolab) that we have recently developed in Matlab (MathWorks Inc., Natick, MA, USA) to measure the longitudinal displacement of the distal wall, the cross-sectional diameter change and the distal wall IMT, throughout the entire cardiac cycle (Zahnd et al. 2010, 2011b, 2011c). This technique exploits the grey-level information of the images and is based on a double-step scheme that relies on robust speckle tracking guided by contour segmentation. The three main steps are detailed below.

### *Initialization phase*

On the first image of each sequence, left and right borders are firstly cut out, with a region of interest (ROI) set approximately 1 cm distal to the carotid bulb and 0.1 cm distal to the right border of the image, representing a covered surface of approximately 1.5 cm wide (Fig. 1a). Then the radial positions of both walls are manually set by indicating, for each wall, another rectangular ROI that must include the intima-media complex, and a small part of the lumen and of the adventitia. Finally, the rough initial IMT of both walls is manually set by indicating one point of the lumen-intima interface and one point of the media-adventitia interface. Then the full sequence is automatically processed using these initial inputs.

### *Segmentation phase*

The segmentation of the intima-media complex is realized by finding the central skeleton (i.e., the curved line located exactly in between the contours of the two intima-lumen and media-adventitia interfaces [Fig. 1b]). To perform the segmentation, a spatial transformation  $T$  is first applied on the current image, using the position of the skeleton of the previous frame, to represent the curved interfaces to be segmented by horizontal lines. With this transformation  $T$ , the previous skeleton is represented as a straight line and the corresponding translation is applied to the image column by column. Then, a vertical matched filter  $H$ , defined as the convolution of the first derivative of a Gaussian (length of 7 pixels, standard deviation of 0.4) with a pair of diracs separated by a distance  $\Delta$ , is applied to highlight the typical double-line pattern of the horizontal interfaces, characterized by two high gradient values distant from the length of the IMT (Zahnd et al. 2011b). The central value of  $\Delta$  corresponds to the average IMT and is determined in the  $n$ -th frame by its value in the previous frame. The convolution filter  $H$  is applied iteratively with seven different values of  $\Delta_i$  to take into account the tiny changes of the IMT along the cardiac cycle (Selzer et al. 2001) and for each pixel, the output with the higher value is kept and the corresponding IMT value  $\Delta_i$  is memorized. The output of the  $H$  filter is a velocity map that represents all the position probabilities of the skeleton. A front propagation approach with an upwind scheme technique (Cohen 2005) is then applied on this map to build a cost function, and the optimal path with the minimal cost is finally calculated by gradient descent from the left and right sides to the center. The inverse spatial transformation  $T^{-1}$  is then applied to the optimal path to match back the initial image, and the skeleton of the current frame is finally calculated by a 2-degree polynomial approximation of the optimal path, to represent a realistic smooth contour. The two contours of the lumen-intima and the media-adventitia interfaces are positioned at a distance of  $\Delta_i/2$  from the skeleton for visual confirmation.

All the successive positions of the skeleton through the sequence are used to measure the radial trajectory of the wall, as well as to provide a position a priori for the longitudinal speckle tracking scheme. The cross-sectional diameter for each frame of the sequence is estimated as the median

distance between the near and far walls, using the previously segmented contours. Carotid artery distensibility is defined as the relative diameter change for a pressure increment and calculated as: arterial distensibility =  $\Delta D/(\Delta P \times D)$ , with  $\Delta D$  the total amplitude of the cross-sectional diameter change,  $\Delta P$  the blood pressure, and  $D$  the maximal cross-sectional diameter; and thus, expressed in units  $10^{-3} \text{ mmHg}^{-1}$  (O'Rourke et al. 2002). The carotid IMT is also measured at end-diastole in the left common carotid, as the median distance between the lumen-intima and media-adventitia interfaces derived from the temporally corresponding  $\Delta$  value of the segmentation process.

### *Speckle tracking phase*

Speckle tracking, also called block matching, is a widely used technique to assess the motion in ultrasound B-mode sequences (Yeung et al. 1998). This method consists in selecting a small block of pixels in an image and finding its most probable position in the next image by determining the most similar corresponding block. We propose here an enhanced version of speckle tracking, well suited to the need of robustness of a large in vivo study, which exploits an a priori position guidance combined to the collaboration of multiple blocks (Zahnd et al. 2010). First, the previously estimated skeleton (that is to say the intima-media centerline) is used as a radial a priori and a group of 16 blocks of dimensions  $1.5 \times 0.3 \text{ mm}^2$  are automatically and regularly positioned in the image (Fig. 1c), within search windows of dimension  $2.13 \times 0.63 \text{ mm}^2$ . The blocks are located inside the intima-media complex and just adjacent to the intima-lumen interface. Then, the image is interpolated by a factor 10 and the speckle tracking operation is computed independently for each block using the normalized sum of squared differences (NSSD) criterion. Finally, the resulting displacement between the considered pair of frames is calculated by robust statistics as the median value of the individual result from all the 16 blocks. In summary, this approach has two main advantages: first, the blocks are always repositioned along the skeleton in the current image and, therefore, cannot generate a cumulative drift error through the sequence; and second, the motion estimation is realized by considering a set of several points defining a more global zone of the wall and rejecting the outliers and, therefore, does not depend on a specific local point that can temporarily suffer from weak echoes, out-of-plane movements or motion artifacts.

The longitudinal trajectory of the wall tissues along the complete sequence is calculated by summing up all the previously estimated longitudinal displacements between two consecutive frames. A carotid longitudinal displacement index is then calculated to provide a measure of carotid longitudinal displacement per 10 mm Hg change in arterial pulse pressure, as: carotid longitudinal index =  $\Delta X/(10 \times \Delta P)$ , with  $\Delta X$  the total amplitude of the longitudinal motion and  $\Delta P$  the blood pressure.

### *Cardiovascular risk measures*

Intra-oral screening for periodontal disease status was undertaken by a dentist or an oral health therapist. All teeth present in the mouth (excluding third molars) were measured at four sites that included mesio-buccal, mid-buccal, disto-buccal and disto-lingual/palatal. All periodontal recordings were entered into a conventional database (MS Access, 2007 edition). Moderate periodontal disease was defined as the presence of either two sites between adjacent teeth with  $\geq 4 \text{ mm}$  attachment loss or at least two such sites with  $\geq 5 \text{ mm}$  pockets, and severe periodontitis as having at least two sites between adjacent teeth with  $\geq 6 \text{ mm}$  attachment loss and at least one pocket  $\geq 5 \text{ mm}$  (Page and Eke 2007). A computer algorithm programmed into MS Access calculated the number of sites according to the criteria above and confirmed periodontal case status.

The methods for assessing the other cardiovascular risk factors in the periodontal disease group are described elsewhere (Skilton et al. 2011). In brief, glycated hemoglobin (HbA1c) was measured by

turbidimetric inhibition immunoassay with a COBAS INTEGRA (Roche Diagnostics, Indianapolis, IN, USA), non-fasting total cholesterol by enzymatic methods and HDL-c was measured directly with an ADVIA chemistry system (Siemens, Tarrytown, NY, USA). NonHDL-c was calculated as total cholesterol, HDL-c. Smoking status and diabetes were derived from a self-administered questionnaire. Two participants with missing data concerning smoking status have been grouped with those who refused to answer the smoking-related questions. Carotid-dorsalis pedis PWV was measured by applanation tonometry (SphygmoCor-PVMx device, AtCor Medical, Sydney, Australia). Seated blood pressure was measured three times, with 3 min between readings, using an automated device (Welch Allyn Medical Products, Skaneateles Falls, NY, USA). The average of the final two recordings was used. Supine blood pressures were obtained immediately after acquisition of both the left and right carotid ultrasounds for use in the calculation of arterial stiffness measures. One participant was missing the supine blood pressure for the left carotid artery, the supine pressure for the right carotid was used instead; and another was missing both supine blood pressures, the seated blood pressure was used.

For the control group, biochemical analysis was undertaken with an Abbott Automat (Abbott, Rungis, France), within the University Hospital of Lyon clinical laboratory. Supine blood pressure was measured with an automated device (OMRON M3, Rosny Sous Bois, France), at the end of carotid examination on the left arm. The lowest of three recordings was used. Data concerning age, sex, height and weight, smoking status and treatment were collected by the same investigator (M.D.).

### *Statistical analysis*

Neither longitudinal displacement of the carotid artery wall, nor its ratio with pulse pressure—the carotid longitudinal displacement index—were normally distributed and, thus, were natural log transformed prior to analysis. Group comparisons were made using Student's t-test for continuous variables and c2 analysis for nominal variables. As previously described, information from both left and right carotid arteries was available for the periodontal disease group, however, only the left side was available for the control group, because of the independent clinical study protocols. Therefore, for each participant in the periodontal disease group, the amplitude of the longitudinal displacement was calculated by averaging the amplitude from the left and right carotid arteries and used for analysis within the periodontal disease group, whereas only data for the left carotid artery were used for comparative analysis involving both groups. Carotid longitudinal displacement and cross-sectional distensibility were assessed a second time in 20 randomly selected participants from the periodontal disease group and intraobserver reproducibility was determined by means of intraclass correlations coefficients. The association of carotid longitudinal displacement with cardiovascular risk factors was assessed in the periodontal disease group, first by Pearson correlation, followed by multivariable linear regression models adjusting for (1) age and sex, and (2) other risk factors. The selection of variables in this second model was based on those variables with the strongest association (i.e., with statistical significance in the univariate model) for each category of variables (anthropometry [i.e., external morphological characteristics, as for example waist or BMI], blood pressure, lipids, diabetes and periodontal disease), as derived from the previous model. Associations of risk factors with carotid longitudinal displacement derived from multivariable models are presented as standardized b-coefficients. All statistical analysis was undertaken using IBM SPSS Statistics (v. 19.0; IBM Corp., Somers, NY, USA). Statistical significance was inferred at  $2 p < 0.05$ .

## **RESULTS**

Participant characteristics for the periodontal disease group and the control group are shown in Table 1. Briefly, the periodontal disease group was at higher overall cardiovascular risk (i.e., had markedly increased adiposity, lower HDL-c, a high prevalence of diabetes, higher rates of smoking and raised

HbA1c levels).

The proposed Carolab method was used to assess the wall two-dimensional (2-D) trajectory and the IMT on each subject, as previously described. The accuracy of the lumen-intima and media-adventitia interfaces resulting from the segmentation process was visually confirmed for each sequence by an experienced observer (G.Z.). The longitudinal trajectory of the far wall of the common carotid artery and the cross-sectional variation of the diameter was assessed for all available cardiac cycles. Representative tracings of the longitudinal displacement and the cross-sectional diameter change from participants in the periodontal disease group and subjects in the control group are presented in Figure 2. Individual cardiac cycles with longitudinal and cross-sectional tracings of insufficient quality (i.e., not presenting a reproducible cyclic motion, mostly for the periodontal group, with an approximate occurrence of about one cycle on three) were discarded prior to averaging the remaining cycles.

Results of the comparative measures between the two populations for the longitudinal displacement index, the cross-sectional distensibility and the IMT are presented in Figure 3. The periodontal disease group had significantly greater subclinical atherosclerosis than controls (carotid IMT: 0.64 mm (0.17) vs. 0.57 mm (0.09);  $p = 0.007$ , Fig. 3c). Most importantly, carotid longitudinal displacement was markedly lower in the periodontal disease group than the control group (geometric mean [interquartile range]: 0.15 mm (0.13) vs. 0.42 mm (0.30);  $p < 0.0001$ ), as was the carotid longitudinal displacement index (Fig. 3a). This remained after adjustment for cardiovascular risk factors (adjusted for age, sex, smoking status, BMI, HDL-c, nonHDL-c, HbA1c and diastolic blood pressure (DBP);  $p < 0.0001$ ) and further adjustment for cross-sectional distensibility and carotid IMT ( $p < 0.0001$ ). Interestingly, there was no difference between groups for the cross-sectional distensibility measure (Fig. 3b).

The intraobserver intraclass correlation coefficients for the raw carotid longitudinal displacement measure, and the carotid longitudinal displacement index, were 0.959 and 0.971, respectively. Carotid longitudinal displacement index correlated with carotid IMT ( $r = 2.200$ ,  $p = 0.01$ ) and carotid cross-sectional distensibility ( $r = .317$ ,  $p < 0.0001$ ) but not PWV ( $r = 2.064$ ,  $p = 0.49$ ; periodontal disease group only).

To describe the risk factors for carotid longitudinal displacement index in those with periodontal disease, we determined crude correlations, age- and sex-adjusted associations and multivariable associations, with cardiovascular risk factors (Table 2). The results of the multivariable model were similar after exclusion of participants with only post-randomization data available (age: b-coefficient = 2.228,  $p = 0.04$ ; BMI: b-coefficient = 2.527,  $p < 0.0001$ ), or further adjustment for carotid distensibility (age: b-coefficient = 2.257,  $p = 0.009$ ; BMI: b-coefficient = 2.458,  $p < 0.0001$ ) or PWV (age: b-coefficient = 2.216,  $p = 0.04$ ; BMI: b-coefficient = 2.501,  $p < 0.0001$ ). When the raw carotid longitudinal displacement measure was modeled, instead of the index that incorporates pulse pressure, results showed that SBP, DBP and pulse pressure were not associated in crude or age and sex-adjusted models ( $p > 0.10$  for all comparisons), however, the strongest correlates in the multivariable model were age (b-coefficient = 2.235,  $p = 0.03$ ), waist (b-coefficient = 2.357,  $p = 0.001$ ) and pulse pressure (b-coefficient = .175,  $p = 0.07$ ).

## DISCUSSION

In this study, we have presented an approach based on robust speckle tracking guided by contour segmentation, aiming at the estimation of the arterial wall 2-D motion. Using this method, we have demonstrated that the amplitude of the longitudinal displacement of the carotid arterial wall may be a significant marker of cardiovascular risk, as it is markedly reduced in Indigenous Australians with

periodontal disease compared with a healthy Caucasian control population. Compared with this latter group, the at-risk participants had a higher prevalence of smoking and diabetes, elevated levels of adiposity and HbA1c, and lower HDL-c. However, the impairment of carotid longitudinal displacement was independent of these established cardiovascular risk factors, and also of cross-sectional distensibility and carotid IMT. This suggests that the longitudinal displacement may represent an independent complementary marker of vascular health and disease.

There are only a few published reports describing the longitudinal displacement of arterial walls. The first in vivo demonstration, in pigs, used small piezoelectric crystals sutured onto the artery and showed a distinct longitudinal displacement of about half the amplitude of the diameter change (Tozzi et al. 2001). A variety of ultrasound-based approaches have then been used in humans to assess arterial longitudinal displacement, including: an echo-tracking method (Persson et al. 2003; Cinthio et al. 2005, 2006; Cinthio and Ahlgren 2010); different block-matching approaches (Golemati et al. 2003; Gastouniotti et al. 2011; Larsson et al. 2011; Zahnd et al. 2011a), and the Velocity Vector Imaging commercial software (VVI, Research Arena 2; TomTec imaging systems GmbH, Unterschleissheim, Germany) (Svedlund and Gan 2011b). We have recently proposed a novel segmentation and guided speckle tracking-based method to assess the 2-D movement of the arterial walls (Zahnd et al. 2010, 2011b, 2011c). Numerous approaches have been proposed to segment the carotid artery walls, using active contours (Loizou et al. 2007), local statistics (Delsanto et al. 2007), dynamic programming (Cheng and Jiang 2008) or gradient (Faita et al. 2008). However, these methods usually process single images rather than sequences and provide information related to the radial direction (i.e., IMT and cross-sectional diameter, but do not permit to assess the wall longitudinal motion. The method presented here combines speckle tracking to guidance by contours segmentation, as proposed in (Destrempe et al. 2011).

As previously noted, carotid longitudinal displacement is reduced in patients with carotid plaques (Svedlund and Gan 2011a). Aging was a strong, and inverse, correlate of longitudinal displacement in the current study, suggesting that differences in age may have confounded prior studies demonstrating impaired carotid longitudinal displacement in older adults with coronary artery disease and type 2 diabetes (Svedlund and Gan 2011b; Zahnd et al. 2011a). Recently, a study showed that longitudinal displacements of the porcine carotid artery undergoes profound changes in response to catecholamines and accompanying effects on blood pressure, constituting a possible link between mental stress and cardiovascular disease (Ahlgren et al. 2011). Importantly, longitudinal displacement of the carotid wall has recently been demonstrated to be predictive of incident cardiovascular events in high-risk subjects, independent of cross-sectional carotid stiffness and carotid IMT (Svedlund et al. 2011). This is consistent with our findings and suggests that the noninvasive assessment of carotid longitudinal displacement may provide information concerning vascular disease and risk of cardiovascular events that is otherwise not captured by other measures of carotid stiffness and structure.

Adiposity was also strongly, and inversely associated with carotid longitudinal displacement, independent of other risk factors. Approximately 67% of the cardiovascular risk associated with obesity is mediated via established cardiovascular risk factors (Wilson et al. 2008), however, whether or not impaired carotid longitudinal displacement contributes to the excess cardiovascular risk associated with obesity is unknown, but may be a topic of future study. Blood pressure was the other major determinant of carotid longitudinal displacement, although this association was markedly weakened when incorporated into a multivariable model with BMI, consistent with our previous findings for carotid IMT (Skilton et al. 2008).

We suggest that periodontal disease per se may possibly be related to the arterial longitudinal

displacement. Periodontal disease is an emerging cardiovascular risk factor associated with impaired endothelial function and increased subclinical atherosclerosis (Amar et al. 2003; Scannapieco et al. 2003; Bouchard et al. 2010; Beck et al. 2011; Skilton et al. 2011), putatively via a shared pathogenic inflammatory response (Offenbacher et al. 2005). The periodontal disease group was made up of Indigenous Australians, who are at increased risk of premature cardiovascular disease, predominantly because of increased burden of established and emerging cardiovascular risk factors, as opposed to being Indigenous per se (O'Dea 1991; Brown et al. 2005). Thus, the reduced carotid longitudinal displacement in the periodontal group independent of established risk factors, suggests that periodontal disease may influence carotid longitudinal displacement. Other cultural and ethnic differences, and factors such as socioeconomic disadvantage and psychosocial stress, may have contributed to the observed differences between those with periodontal disease and the control group. Although as previously noted, these are not major contributors to Indigenous cardiovascular health and disease beyond their associations with established risk factors. Moreover, while the periodontal status of the control group is unknown, it is likely that some of the control group had moderate to severe periodontal disease given the population prevalence of periodontal disease in France (Bourgeois et al. 2007). Accordingly, the true association of periodontal disease with carotid longitudinal displacement may be stronger than that observed in this study.

The periodontal disease group in our study had increased carotid IMT, an established measure of arterial structure that is independently associated with incident cardiovascular events (Lorenz et al. 2007), indicative of this group having poorer vascular health and being at increased cardiovascular risk. While this was mirrored by the carotid longitudinal displacement measure, carotid cross-sectional stiffness did not differ by periodontal disease status. This is consistent with a recent study that found no difference in PWV by periodontal disease status (Franek et al. 2009). These differences between the longitudinal, cross-sectional and PWV measures may be because of the differing structural properties that determine arterial axial and circumferential stretch, with the former being putatively under greater local control related to the deposition of collagen, smooth muscle proliferation and hypertrophy and breakdown of elastin (Dobrin et al. 1990; Humphrey et al. 2009). Indeed, there was no significant association between longitudinal displacement and PWV, considered the gold-standard method for the noninvasive assessment of arterial stiffness. This is consistent with the longitudinal displacement of the walls of the conduit arteries not acting to cushion or slow the arterial pulse wave, unlike cross-sectional distension. Accordingly, longitudinal displacement of the arterial walls may represent a measure of arterial stiffness complementary to cross-sectional distensibility or PWV. An advantage of the ultrasound-derived localized measures of arterial stiffness, as compared to carotid-femoral PWV, is that these methodologies avoid cultural and ethical obstacles regarding accessing the femoral artery in certain populations and subject groups. In addition, these measures can be obtained as part of a brief addendum to a commonly used carotid IMT scanning protocol.

The impaired carotid longitudinal displacement in the periodontal disease group was also independent of subclinical atherosclerosis and arterial stiffness, indicating that carotid longitudinal displacement does not simply replicate information concerning vascular health and disease captured by more established noninvasive techniques for assessing arterial structure and stiffness.

### *Study limitations*

This study raises several limitations that must be considered. First, two different ultrasound machines were used to acquire the images for each population. Moreover, the cardiovascular risk measurement and acquisition protocol were slightly different as the two populations were initially enrolled in two different larger clinical studies in Australia and France, respectively. Also, a significant genetic

difference could have been caused by the disparity in the racial makeup of the two populations, potentially affecting the results. Nevertheless, all measurements were centralized and realized with automated software, and our results are consistent with carotid longitudinal displacement being related to cardiovascular health (Svedlund et al. 2011). Second, some individual cardiac cycles did not present a reproducible pattern cycle and were discarded, the resulting motion amplitude being calculated with the remaining cycles, as detailed previously. Although almost all cycles were reproducible for the healthy subjects, approximately one cardiac cycle per three heart beats was of insufficient quality for the periodontal participants. This degrading phenomenon is known to have multiple possible causes, among which the subject breathing, swallowing, slightly moving, or contracting his neck muscles. Moreover, we did observe more data of lower quality in periodontal participants, potentially because of a higher BMI and, therefore, a poorer tissue echogenicity; or a different ultrasound machine with lower imaging definition. However, while the longitudinal displacement of a carotid B-mode sequence is more difficult to measure than the radial displacement, because of the homogeneity of tissues in that direction, we obtained excellent reproducibility using our speckle tracking method. Third, information regarding the intake of cardiovascular and cardiometabolic drugs is not available in this study and possible confounding effects can, therefore, not be assessed. Similarly, inflammatory markers have not yet been assessed in these participants, and as such we were unable to ascertain whether systemic inflammation is associated with carotid longitudinal displacement. Finally, the blood velocity, which generates a friction corresponding to the wall shear stress at the surface of the endothelium (Davies 2008), is not considered in this work. However, the wall longitudinal motion may not be principally caused by this single tangential force, as other contribution forces are likely of greater importance. Longitudinal arterial movement is indeed thought to be coupled mostly with radial displacement (i.e., longitudinal displacement induced by radial systolic stretching, or radial mechanically induced longitudinal displacement), with only wall shear stress being a relatively minor contributor (Hodis and Zamir 2011). We propose that for large elastic arteries, such as the common carotid artery, the wall longitudinal displacement may be induced by a first protosystolic backward motion caused by the apical motion of the aortic valve annulus, and a second mesosystolic backward motion caused by the reflected wave.

## **SUMMARY**

Carotid longitudinal displacement, i.e., the longitudinal movement of the arterial wall during the cardiac cycle, is potentially an alternative and/or complementary measure to other noninvasive measures of arterial health. In this study, we have presented a specific speckle tracking approach guided by contour segmentation, dedicated to assess the carotid wall 2-D displacement in ultrasound B-mode in vivo sequences. Furthermore, we have shown that carotid longitudinal displacement is reduced in Indigenous Australians with periodontal disease compared with a Caucasian group at low cardiovascular risk, independent of established cardiovascular risk factors, cross-sectional carotid stiffness and subclinical carotid atherosclerosis. The strongest correlates of carotid longitudinal displacement in those with periodontal disease were aging, adiposity and blood pressure. Accordingly, carotid longitudinal displacement may provide information concerning the vascular abnormalities that accompany cardiovascular risk factors complementary to that obtained from existing noninvasive methodologies.

## *Acknowledgments*

The authors gratefully acknowledge the support of PerioCardio study participants, study staff, Danila Dilba Health Services, Northern Territory Oral Health Service, Northern Territory Correctional Services, and Wurli Wurlinjang Aboriginal Health Service. The PerioCardio Study was funded by the

National Health and Medical Research Council of Australia (NHMRC, Project Grant #627100). L.M.J. is supported by NHMRC Career Development Award #565260. L.M.B. is supported by NHMRC fellowship #605837. M.R.S. is supported by NHMRC fellowship #1004474.

## FIGURES

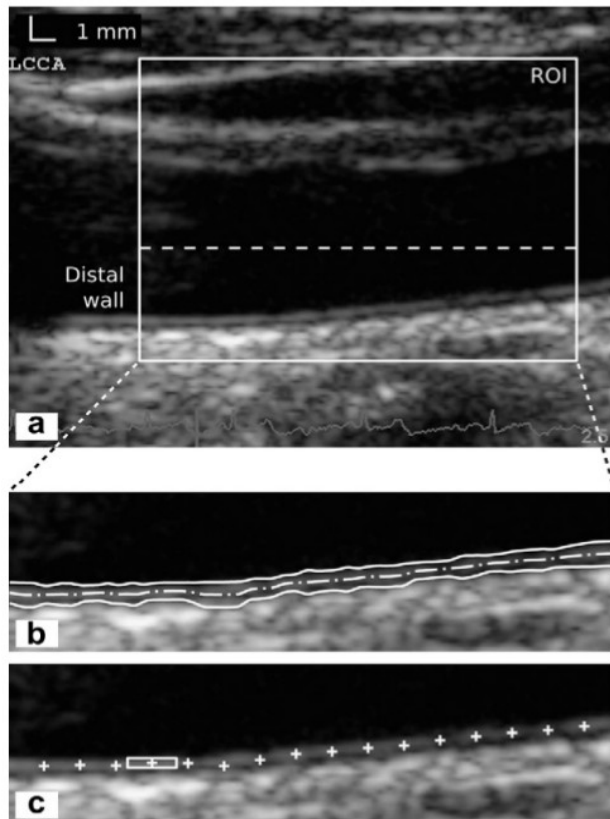


Fig. 1. Schematic view of longitudinal displacement method. (a) Position of the region-of-interest (ROI) in the image. (b) Result of the segmentation of the distal wall with the central skeleton (dash-dotted) and the two interface contours of the intima-media complex (solid). (c) Position of the 16 speckle tracking blocks along the wall for the longitudinal motion estimation.

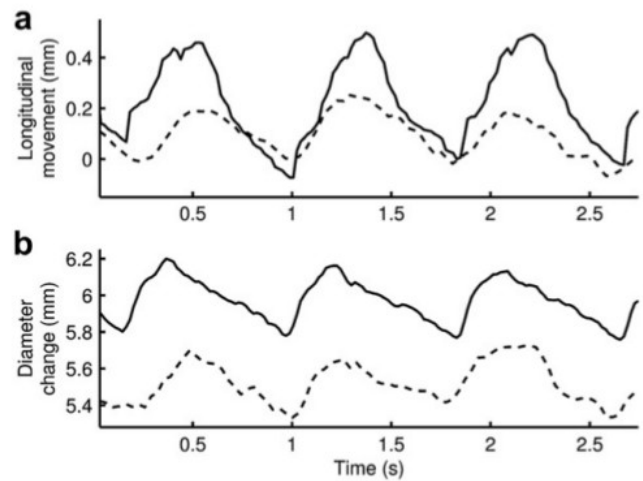


Fig. 2. Longitudinal displacement (a) and cross-sectional diameter change (b) of the arterial wall during three consecutive cardiac cycles, from representative participants in the periodontal disease group (dashed) and subjects in the control group (solid).

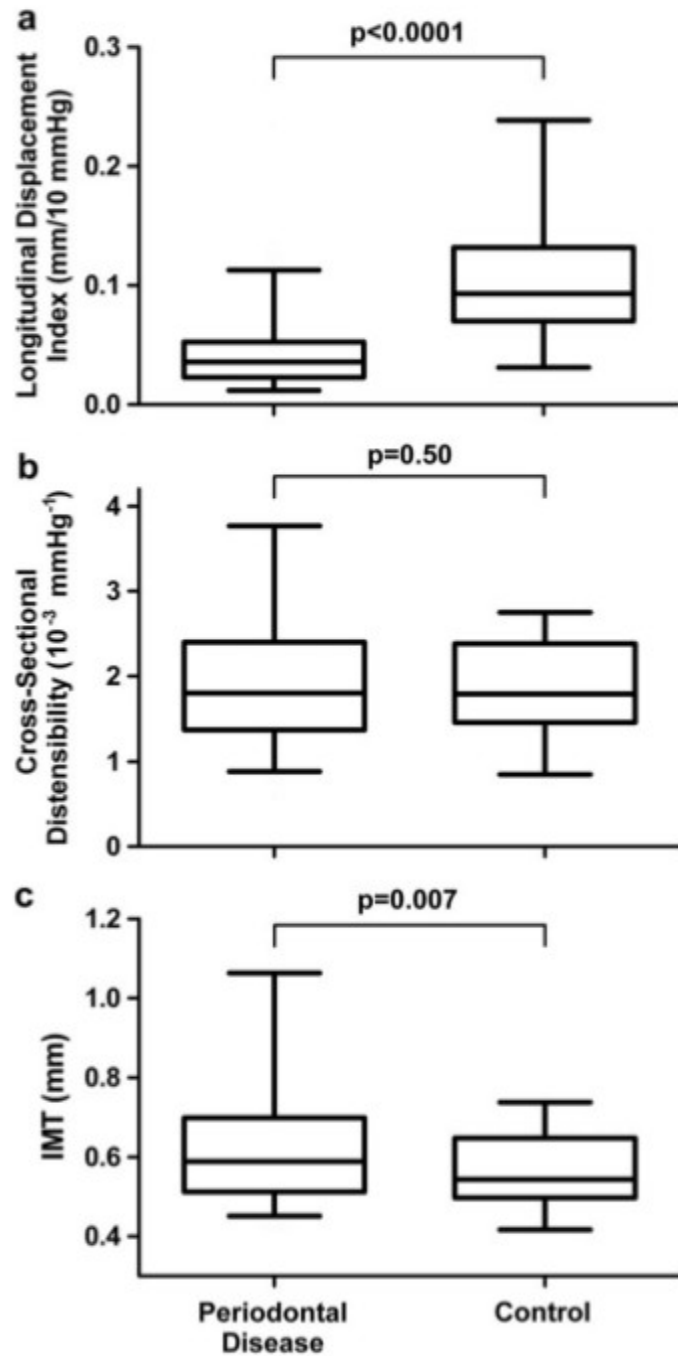


Fig. 3. Carotid longitudinal displacement index (a), cross-sectional distensibility (b) and intima-media thickness (IMT) (c) in indigenous Australians with periodontal disease and healthy control subjects. Box, line and error bars represent 5th, 25th, 50th (median) 75th, and 95th percentiles. The  $p$  values for the longitudinal displacement index and cross-sectional distensibility correspond to the derived Ln-transformed data.

## TABLES

Table 1. Participant characteristics

	Periodontal disease (n = 125)	Control (n = 27)	p value
Age, year	43.8 (10.8)	45.3 (7.0)	0.37
Sex-male, n (%)	48 (38%)	12 (44%)	0.56
Smoking, n (%)			
Never	27 (22%)	19 (70%)	<0.0001
Current	64 (51%)	0 (0%)	
Ex	25 (20%)	8 (30%)	
Refused or missing	9 (7%)	0 (0%)	
BMI, kg/m <sup>2</sup>	30.1 (7.5)	22.7 (2.7)	<0.0001
Waist, cm	102 (14)	85 (8)	<0.0001
Total cholesterol, mmol/L	5.10 (1.09)	5.36 (1.04)	0.27
HDL-c, mmol/L	1.14 (0.31)	1.58 (0.35)	<0.0001
NonHDL-c, mmol/L	3.96 (1.09)	3.78 (1.13)	0.45
HbA1c, %	6.3 (1.5)	5.5 (0.3)	<0.0001
Diabetes, n (%)	17 (14%)	0 (0%)	0.04
SBP, mm Hg	125 (18)	121 (12)	0.29
DBP, mm Hg	80 (10)	75 (12)	0.03
PP, mm Hg	45 (13)	46 (10)	0.72
PWV, m/s	8.4 (1.3)	–	–

BMI = body mass index; SBP = systolic blood pressure; DBP = diastolic blood pressure; PP = pulse pressure; PWV = pulse wave velocity; HbA1c = glycosylated hemoglobin; HDL-c = high-density lipoprotein cholesterol.

Table 2. Association of cardiovascular risk factors with the carotid longitudinal displacement index in participants with periodontal disease

	Unadjusted		Age- and sex-adjusted		Multivariable model	
	$\beta$ -coefficient	p value	$\beta$ -coefficient	p value	$\beta$ -coefficient	p value
Age	-.345	<0.0001	-.363	<0.0001	-.256	0.01
Sex	-.074	0.41	-.127	0.14	-.122	0.19
Smoking						
Never	.000	referent	.000	referent	.000	referent
Current	.176	0.13	.122	0.27	-.100	0.40
Ex	-.024	0.83	-.015	0.89	-.213	0.06
Missing	-.023	0.81	-.035	0.71	-.175	.08
BMI	-.354	<0.0001	-.287	0.0009	-.479	<.0001
Waist	-.378	<0.0001	-.282	0.002		
Total cholesterol	.018	0.86	-.022	0.81		
HDL-c	.033	0.74	.027	0.77	-.091	0.33
NonHDL-c	.008	0.93	-.029	0.75	-.065	0.47
HbA1c	-.082	0.40	-.022	0.82		
Diabetes	-.040	0.66	.071	0.43	.147	0.13
SBP	-.270	0.002	-.204	0.02	-.079	0.40
DBP	-.206	0.02	-.182	0.03		
Periodontal disease severity	.028	0.75	.003	0.97	.025	0.79

BMI = body mass index; SBP = systolic blood pressure; DBP = diastolic blood pressure; HbA1c = glycosylated hemoglobin; HDL-c = high-density lipoprotein cholesterol.

## REFERENCES

- Ahlgren AR, Cinthio M, Steen S, Nilsson T, Sjoberg T, Persson HW, Lindstrom K. The longitudinal displacement and intramural shear strain of the porcine carotid artery undergo profound changes in response to catecholamines. *Am J Physiol* 2011;302:H1102–H1115.
- Amar S, Gokce N, Morgan S, Loukideli M, Van Dyke T, Vita JA. Periodontal disease is associated with brachial artery endothelial dysfunction and systemic inflammation. *Arterioscler Thromb Vasc Biol* 2003;23:1245–1249.
- Beck JD, Elter JR, Heiss G, Couper D, Mauriello SM, Offenbacher S. Relationship of periodontal disease to carotid artery intima-media wall thickness. *Arterioscler Thromb Vasc Biol* 2011;21:1816–1822.
- Bouchard P, Boutouyrie P, D’Aiuto F, Deanfield J, Deliargyris E, Fernandez-Aviles F, Hughes F, Madianos P, Renvert S, Sanz M. European workshop in periodontal health and cardiovascular disease consensus document. *Eur Heart J Suppl* 2010;12:B13–B22.
- Bourgeois D, Bouchard P, Mattout C. Epidemiology of periodontal status in dentate adults in France, 2002–2003. *J Periodontal Res* 2007;42:219–227.
- Brown A, Walsh W, Lea T, Tonkin A. What becomes of the broken hearted? Coronary heart disease as a paradigm of cardiovascular disease and poor health among indigenous Australians. *Heart Lung Circ* 2005;14:158–162.
- Buhlin K, Gustafsson A, Pockley AG, Frostegard J, Klinge B. Risk factors for cardiovascular disease in patients with periodontitis. *Eur Heart J* 2003;24:2099–2107.
- Celermajer DS, Sorensen KE, Gooch VM, Spiegelhalter DJ, Miller OI, Sullivan ID, Lloyd JK, Deanfield JE. Non-invasive detection of endothelial dysfunction in children and adults at risk of atherosclerosis. *Lancet* 1992;340:1111–1115.
- Cheng D, Jiang X. Detections of arterial wall in sonographic artery images using dual dynamic programming. *IEEE Trans Info Tech Biomed* 2008;12:792–799.
- Cinthio M, Ahlgren AR. Intraobserver variability of longitudinal displacement and intramural shear strain measurements of the arterial wall using ultrasound noninvasively in vivo. *Ultrasound Med Biol* 2010;36:697–704.
- Cinthio M, Ahlgren AR, Bergkvist J, Jansson T, Persson HW, Lindstrom K. Longitudinal movements and resulting shear strain of the arterial wall. *Am J Physiol* 2006;291:H394–H402.
- Cinthio M, Ahlgren AR, Jansson T, Eriksson A, Persson HW, Lindstrom K. Evaluation of an ultrasonic echo-tracking method for measurements of arterial wall movements in two dimensions. *IEEE Trans Ultrason Ferroelectr Freq Control* 2005;52:1300–1311.
- Cohen L. Minimal paths and fast marching methods for image analysis. *Mathematical Models in Computer Vision: The Handbook*. New York: Springer, 2005;97–111.

- Davies P. Hemodynamic shear stress and the endothelium in cardiovascular pathophysiology. *Nat Clin Pract Cardiovasc Med* 2008;6:16–26.
- Delsanto S, Molinari F, Giustetto P, Liboni W, Badalamenti S, Suri J. Characterization of a completely user-independent algorithm for carotid artery segmentation in 2-D ultrasound images. *IEEE Trans Instrum Meas* 2007;56:1265–1274.
- Destrempe F, Meunier J, Giroux M, Soulez G, Cloutier G. Segmentation of plaques in sequences of ultrasonic B-mode images of carotid arteries based on motion estimation and a Bayesian model. *IEEE Trans Biomed Eng* 2011;58:2202–2211.
- Dobrin PB, Schwarcz TH, Mrkvicka R. Longitudinal retractive force in pressurized dog and human arteries. *J Surg Res* 1990;48:116–120.
- Dolan E, Thijs L, Li Y, Atkins N, McCormack P, McClory S, O'Brien E, Staessen JA, Stanton AV. Ambulatory arterial stiffness index as a predictor of cardiovascular mortality in the Dublin Outcome Study. *Hypertension* 2006;47:365–370.
- Faita F, Gemignani V, Bianchini E, Giannarelli C, Ghiadoni L, Demi M. Real-time measurement system for evaluation of the carotid intima-media thickness with a robust edge operator. *J Ultrasound Med* 2008;27:1353–1361.
- Franek E, Klamczynska E, Ganowicz E, Blach A, Budlewski T, Gorska R. Association of chronic periodontitis with left ventricular mass and central blood pressure in treated patients with essential hypertension. *Am J Hypertens* 2009;22:203–207.
- Gamble G, Zorn J, Sanders G, MacMahon S, Sharpe N. Estimation of arterial stiffness, compliance, and distensibility from M-mode ultrasound measurements of the common carotid artery. *Stroke* 1994;25:11–16.
- Gastouniotti A, Golemati S, Stoitsis J, Nikita KS. Comparison of Kalman-filter-based approaches for block matching in arterial wall motion analysis from B-mode ultrasound. *Meas Sci Technol* 2011; 22:114008.
- Golemati S, Sassano A, Lever MJ, Bharath AA, Dhanjil S, Nicolaides AN. Carotid artery wall motion estimated from B-mode ultrasound using region tracking and block matching. *Ultrasound Med Biol* 2003;29:387–399.
- Hansen F, Mangell P, Sonesson B, Lanne T. Diameter and compliance in the human common carotid artery—variations with age and sex. *Ultrasound Med Biol* 1995;21:1–9.
- Hodis Z, Zamir M. Coupled radial and longitudinal displacements and stresses within the arterial wall in pulsatile flow under tethered and free-wall conditions. *Phys Rev E* 2011;83:051923.
- Humphrey JD, Eberth JF, Dye WW, Gleason RL. Fundamental role of axial stress in compensatory adaptations by arteries. *J Biomech* 2009;42:1–8.
- Jiang Y, Kohara K, Hiwada K. Association between risk factors for atherosclerosis and mechanical forces in carotid artery. *Stroke* 2000;31:2319–2324.

Larsson M, Kremer F, Claus P, Kuznetsova T, Brodin LA, D'hooge J. Ultrasound-based radial and longitudinal strain estimation of the carotid artery: A feasibility study. *IEEE Trans Ultrason Ferroelectr Freq Control* 2011;58:2244–2251.

Laurent S, Boutouyrie P, Asmar R, Gautier I, Laloux B, Guize L, Ducimetiere P, Benetos A. Aortic stiffness is an independent predictor of all-cause and cardiovascular mortality in hypertensive patients. *Hypertension* 2001;37:1236–1241.

Loizou C, Pattichis C, Pantziaris M, Tyllis T, Nicolaidis A. Snakes based segmentation of the common carotid artery intima media. *Med Biol Eng Comput* 2007;45:3549–2007.

Lorenz MW, Markus HS, Bots ML, Rosvall M, Sitzer M. Prediction of clinical cardiovascular events with carotid intima-media thickness: A systematic review and meta-analysis. *Circulation* 2007;115:459–467.

Miyaki K, Masaki K, Naito M, Naito T, Hoshi K, Hara A, Tohyama S, Nakayama T. Periodontal disease and atherosclerosis from the viewpoint of the relationship between community periodontal index of treatment needs and brachial-ankle pulse wave velocity. *BMC Public Health* 2006;6:131.

O'Dea K. Cardiovascular disease risk factors in Australian Aborigines. *Clin Exp Pharmacol Physiol* 1991;18:85–88.

O'Rourke MF, Staessen JA, Vlachopoulos C, Duprez D, Plante GE. Clinical applications of arterial stiffness: Definitions and reference values. *Am J Hypertens* 2002;15:426–444.

Offenbacher S, Elter JR, Lin D, Beck JD. Evidence for periodontitis as a tertiary vascular infection. *J Int Acad Periodontol* 2005;7:39–48.

Page R, Eke PI. Case definitions for use in population-based surveillance of periodontitis. *J Periodontol* 2007;78:1387–1139.

AR, Jansson T, Eriksson A, Persson HW, Persson M, Ahlgren Lindstrom K. A new noninvasive ultrasonic method for simultaneous measurements of longitudinal and radial arterial wall movements: First in vivo trial. *Clin Physiol Funct Imaging* 2003;23: 247–251.

Scannapieco FA, Bush RB, Paju S. Associations between periodontal disease and risk for atherosclerosis, cardiovascular disease, and stroke. A systematic review. *Ann Periodontol* 2003;8:38–53.

Selzer RH, Mack WJ, Lee PL, Kwong-Fu H, Hodis HN. Improved common carotid elasticity and intima-media thickness measurements from computer analysis of sequential ultrasound frames. *Atherosclerosis* 2001;154:185–193.

Skilton M, Maple-Brown L, Kapellas K, Celermajer D, Bartold M, Brown A, O'Dea K, Slade G, Jamieson L. The effect of a periodontal intervention on cardiovascular risk markers in Indigenous Australians with periodontal disease: The PerioCardio study. *BMC* 2011; 11:729.

Skilton M, Sieveking D, Harmer J, Franklin J, Loughnan G, Nakhla S, Sullivan D, Caterson I,

Celermajer D. The effects of obesity and non-pharmacological weight loss on vascular and ventricular function and structure. *Diabetes Obes Metab* 2008;10:874–884.

Svedlund S, Eklund C, Robertsson P, Lomsky M, Gan LM. Carotid artery longitudinal displacement predicts 1-year cardiovascular outcome in patients with suspected coronary artery disease. *Arterioscler Thromb Vasc Biol* 2011;31:1668–1674.

Svedlund S, Gan LM. Longitudinal common carotid artery wall motion is associated with plaque burden in man and mouse. *Atherosclerosis* 2011a;217:120–124.

Svedlund S, Gan LM. Longitudinal wall motion of the common carotid artery can be assessed by velocity vector imaging. *Clin Physiol Funct Imaging* 2011b;31:32–38.

Tozzi P, Hayoz D, Oedman C, Mallabiabarrena I, Von Segesser LK. Systolic axial artery length reduction: An overlooked phenomenon in vivo. *Am J Physiol* 2001;280:H2300–H305.

Weber T, Auer J, O'Rourke MF, Kvas E, Lassnig E, Berent R, Eber B. Arterial stiffness, wave reflections, and the risk of coronary artery disease. *Circulation* 2004;109:184–189.

Whincup PH, Gilg JA, Donald AE, Katterhorn M, Oliver C, Cook DG, Deanfield JE. Arterial distensibility in adolescents: The influence of adiposity, the metabolic syndrome, and classic risk factors. *Circulation* 2005;112:1789–1797.

Wilson PW, Bozeman SR, Burton TM, Hoaglin DC, Ben-Joseph R, Pashos CL. Prediction of first events of coronary heart disease and stroke with consideration of adiposity. *Circulation* 2008;118:124–130.

Wu T, Trevisan M, Genco RJ, Falkner KL, Dorn JP, Sempos CT. Examination of the relation between periodontal health status and cardiovascular risk factors: Serum total and high density lipoprotein cholesterol, C-reactive protein, and plasma fibrinogen. *Am J Epidemiol* 2000;151:273–282.

Yeung F, Levinson S, Parker K. Multilevel and motion model-based ultrasonic speckle tracking algorithms. *Ultrasound Med Biol* 1998; 24:427–442.

Zahnd G, Boussel L, Marion A, Durand M, Moulin P, Sérusclat A, Vray D. Measurement of two-dimensional movement parameters of the carotid artery wall for early detection of arteriosclerosis: A preliminary clinical study. *Ultrasound Med Biology* 2011a;37: 1421–1429.

Zahnd G, Marion A, Sérusclat A, Moulin P, Durand M, Boussel L, Vray D. A new user-independent in vivo method for 2D motion estimation of the carotid wall by ultrasound imaging for early detection of pathological behavior. *IEEE Int Ultrason Symp* 2010;1348–1351.

Zahnd G, Orkisz M, Sérusclat A, Vray D. Minimal-path contours combined with speckle tracking to estimate 2-D displacements of the carotid artery wall in B-mode imaging. *IEEE Int Ultrason Symp* 2011b;732-735.

Zahnd G, Orkisz M, Sérusclat A, Vray D. Estimation de la trajectoire 2-D des parois de l'artère carotide, dans des séquences d'images échographiques, par une approche conjointe de segmentation et de suivi de speckle guidé. *GRETSI* 2011c (in press).